Issue No. 3 · 2026
ADVANCED STUDIES
IN ARCHITECTURE AND CIVIL ENGINEERING
(ASACE)

ISSN 3134-8475 (Print)
ISSN 3134-8483 (Online)

UDC 624.131.537; 624.154; 625.731; 699.841
Research article
https://doi.org/10.51488/3134-8483/3-01

CC BY 4.0

DYNAMIC STABILITY OF PILE-REINFORCED ROAD EMBANKMENT SLOPES: A SMALL-SCALE EXPERIMENTAL STUDY

Aida A. Adiyeva[1], Tatiana S. Baratova[1], Ivan S. Bondar[1]*, Alexander V. Anisimov[2]

[1]Kazakh Automobile and Road Institute named after L.B. Goncharov (KazARI), 050061, Almaty, Republic of Kazakhstan.
[2]Moscow Automobile and Road Construction State Technical University (MADI), Moscow, Russia
*Corresponding author, e-mail: ivan_sergeevich_08@mail.ru

ABSTRACT

Introduction. In seismic regions, the slopes of road embankments must remain stable under dynamic and seismic loads, and the slope is frequently the most vulnerable part of the structure. Piles limit slope deformation by redistributing stresses in the soil–pile–structure system, but experimental data on pile-reinforced slopes under controlled dynamic loading are scarce. **Materials and Methods.** A small-scale model of a loam embankment slope (about 45°, 20 kg surcharge on the crest) was tested on a laboratory vibration platform in two configurations: unreinforced, and reinforced by rows of timber piles with beam-connected heads. The response was measured by three-component digital accelerometers; signals were acquired and processed in ZETLAB. **Results and Discussion.** The unreinforced slope began to slide at an excitation frequency of 8 Hz. At this frequency the reinforced slope remained stable at similar response accelerations (peaks of about 4.0 and 10.1 m/s² along X and Y, versus 4.2 and 10.4 m/s² without reinforcement). Significant deformation of the reinforced slope developed only at about 10 Hz, with peak accelerations of 5.2 and 14.2 m/s². As the force of an unbalanced-mass vibrator is proportional to the square of frequency, the threshold shift from 8 to 10 Hz corresponds to an approximately 1.56-fold increase in excitation intensity. **Conclusions.** Pile-and-beam reinforcement increased the dynamic stability of the model slope and delayed its failure. Since each configuration was tested once at 1g, the numerical values are approximate and need confirmation by repeated tests and calculations. Combined with accelerometer monitoring, physical modelling provides a practical basis for assessing the seismic resistance of transport embankments and planning their monitoring.

KEYWORDS: embankment slopes; slope stability; pile reinforcement; physical model testing; vibration loading; seismic resistance of embankments; dynamic response; accelerometer monitoring.

FOR CITATION:

Adiyeva A.A., Baratova T.S., Bondar I.S., Anisimov A.V. Dynamic stability of pile-reinforced road embankment slopes: a small-scale experimental study. Advanced Studies in Architecture and Civil Engineering. 2026; 1 (3): 4-23. https://doi.org/10.51488/3134-8483/3-01

© Adiyeva A.A., Baratova T.S., Bondar I.S., Anisimov A.V., 2026

Issue No. 3 · 2026
ADVANCED STUDIES
IN ARCHITECTURE AND CIVIL ENGINEERING
(ASACE)

ISSN 3134-8475 (Print)
ISSN 3134-8483 (Online)

ӘОЖ 624.131.537; 624.154; 625.731; 699.841
Ғылыми мақала
https://doi.org/10.51488/3134-8483/3-01

CC BY 4.0

ҚАДАЛАРМЕН АРМИРЛЕНГЕН АВТОМОБИЛЬ ЖОЛЫ ҮЙІНДІЛЕРІ БЕТКЕЙЛЕРІНІҢ ДИНАМИКАЛЫҚ ТҰРАҚТЫЛЫҒЫ: ШАҒЫН АУҚЫМДЫ ЭКСПЕРИМЕНТТІК ЗЕРТТЕУ

Аида А. Адиева[1], Татьяна С. Баратова[1], Иван С. Бондарь[1] *, Александр В. Анисимов[2]
[1]Л.Б. Гончаров атындағы Қазақ автомобиль-жол институты (ҚазАДИ), 050061, Алматы, Қазақстан Республикасы.
[2]Мәскеу автомобиль-жол мемлекеттік техникалық университеті (МАДИ), Мәскеу, Ресей.
*Хат-хабар автор, e-mail: ivan_sergeevich_08@mail.ru

АҢДАТПА
Кіріспе. Сейсмикалық белсенді аудандарда автомобиль жолы үйіндісінің беткейі көбіне құрылыстың ең осал бөлігі болып шығады, сондықтан оның динамикалық, оның ішінде сейсмикалық, әсерлер кезіндегі тұрақтылығы маңызды. Қадалар «топырақ – қада – құрылыс» жүйесіндегі кернеулерді қайта бөліп, беткей деформацияларын азайтады, бірақ армирленген беткейдің бақыланатын динамикалық жүктемеге жауабы туралы тәжірибелік деректер әзірге аз. **Материалдар мен әдістер.** Еңісі шамамен 45°, жотасына 20 кг жүк қойылған саздақ үйінді беткейінің шағын масштабты моделі зертханалық сейсмоплатформада сыналды. Екі нұсқа салыстырылды: армирленбеген беткей және бастары арқалықтармен байланыстырылған ағаш қадалар қатарлары бар беткей. Реакцияны үш компонентті сандық акселерометрлер жазды, сигналдар ZETLAB бағдарламасында өңделді. **Нәтижелер және талқылау.** Армирленбеген беткей қоздыру жиілігі 8 Гц-ке жеткен бойда сырғи бастады. Армирленген беткей осы жиілікте шамалас үдеулерде пішінін сақтады (X және Y осьтері бойынша шекті мәндер шамамен 4,0 және 10,1 м/с², армирленбеген модельде – 4,2 және 10,4 м/с²). Айқын деформациялар тек 10 Гц маңында, шекті үдеулер 5,2 және 14,2 м/с²-ге жеткенде пайда болды. Дебаланстық қоздырғыштың күші жиіліктің квадратына пропорционал өседі, демек шектің 8-ден 10 Гц-ке жылжуы шамамен 1,56 есе қарқындырақ әсерді білдіреді. **Қорытынды.** Нәтижелер қада-арқалықты армирлеудің үйінді беткейінің динамикалық тұрақтылығын арттырып, оның бұзылуын кейінге шегеретінін сапалық тұрғыдан көрсетеді.

ТҮЙІНДІ СӨЗДЕР: үйінді беткейлері; беткей тұрақтылығы; қадалармен армирлеу; модельдік сынақтар; дірілдік жүктеме; үйінділердің сейсмикалық төзімділігі; динамикалық реакция; акселерометрлік мониторинг.
ДӘЙЕКСӨЗ ҮШІН:
Адиева А.А., Баратова Т.С., Бондарь И.С., Анисимов А.В. Қадалармен армирленген автомобиль жолы үйінділері беткейлерінің динамикалық тұрақтылығы: шағын ауқымды эксперименттік зерттеу. Advanced Studies in Architecture and Civil Engineering. 2026; 1 (3): 4-23. https://doi.org/10.51488/3134-8483/3-01

© Адиева А.А., Баратова Т.С., Бондарь И.С., А.В. Анисимов, 2026

Issue No. 3 · 2026
ADVANCED STUDIES
IN ARCHITECTURE AND CIVIL ENGINEERING
(ASACE)

ISSN 3134-8475 (Print)
ISSN 3134-8483 (Online)

УДК 624.131.537; 624.154; 625.731; 699.841
Научная статья
https://doi.org/10.51488/3134-8483/3-01

CC BY 4.0

ДИНАМИЧЕСКАЯ УСТОЙЧИВОСТЬ АРМИРОВАННЫХ СВАЯМИ ОТКОСОВ АВТОДОРОЖНЫХ НАСЫПЕЙ: МАЛОМАСШТАБНОЕ ЭКСПЕРИМЕНТАЛЬНОЕ ИССЛЕДОВАНИЕ

Аида А. Адиева[1], Татьяна С. Баратова[1], Иван С. Бондарь [1] *, Александр В. Анисимов[2]
[1]Казахский автомобильно-дорожный институт им. Л.Б. Гончарова (КазАДИ), 050061, Алматы, Республика Казахстан.
[2]Московский автомобильно-дорожный государственный технический университет (МАДИ), Москва, Россия.
*Автор-корреспондент, e-mail: ivan_sergeevich_08@mail.ru

АННОТАЦИЯ
Введение. Откосы автодорожных насыпей в сейсмически активных районах должны сохранять устойчивость при динамических, в том числе сейсмических, воздействиях, и именно откос нередко оказывается самым уязвимым элементом сооружения. Сваи уменьшают деформации откоса, перераспределяя напряжения в системе «грунт - свая - сооружение», однако опытов, в которых поведение армированного откоса прослеживалось бы при контролируемом динамическом нагружении, пока немного. **Материалы и методы.** На лабораторной сейсмоплатформе испытана маломасштабная модель откоса суглинистой насыпи крутизной около 45° с пригрузкой 20 кг на гребне. Сравнивались два варианта: откос без армирования и откос с рядами деревянных свай, объединенных по головам балками. Отклик модели записывали трехкомпонентными цифровыми акселерометрами, сигналы регистрировали и обрабатывали в ZETLAB. **Результаты и обсуждение.** Неармированный откос начал сползать, как только частота возбуждения достигла 8 Гц. Армированный откос при той же частоте сохранил форму, хотя ускорения отклика были сопоставимы (пиковые значения около 4,0 и 10,1 м/с² по осям X и Y против 4,2 и 10,4 м/с² без армирования). Заметные деформации армированного откоса появились лишь около 10 Гц при пиковых ускорениях 5,2 и 14,2 м/с². Сила дебалансного возбудителя растет пропорционально квадрату частоты, поэтому сдвиг порога с 8 до 10 Гц означает воздействие примерно в 1,56 раза более интенсивное. **Выводы.** Свайно-балочное армирование повысило динамическую устойчивость модельного откоса и отсрочило его разрушение.

КЛЮЧЕВЫЕ СЛОВА: откосы насыпей; устойчивость откосов; свайное армирование; модельные испытания; вибрационное нагружение; сейсмостойкость насыпей; динамический отклик; акселерометрический мониторинг.

ДЛЯ ЦИТИРОВАНИЯ:
Адиева А.А., Баратова Т.С., Бондарь И.С., Анисимов А.В. Динамическая устойчивость армированных сваями откосов автодорожных насыпей: маломасштабное экспериментальное исследование. Advanced Studies in Architecture and Civil Engineering. 2026; 1 (3): 4-23. https://doi.org/10.51488/3134-8483/3-01

© Адиева А.А., Баратова Т.С., Бондарь И.С., А.В. Анисимов, 2026

Issue No. 3 · 2026
ADVANCED STUDIES
IN ARCHITECTURE AND CIVIL ENGINEERING
(ASACE)
ISSN 3134-8475 (Print)
ISSN 3134-8483 (Online)

1 INTRODUCTION

Embankment slopes that carry engineering structures remain a difficult problem in geotechnical practice, and in Kazakhstan the difficulty is compounded by continuous traffic loading and by high seismicity in the south and east of the country. During an earthquake, inertial forces add to the static loads from the self-weight of the soil and the structures. Shear strains grow, and potential slip surfaces can develop where none were critical under static conditions. Cohesion and internal friction of the soil may then be insufficient on their own, and the slope needs engineering reinforcement. How a slope responds depends on soil strength, loading, drainage, the deformation mechanism and the way the reinforcement interacts with the surrounding soil [1–5, 17].

Pile reinforcement is one of the established ways to stabilize such slopes. A pile that crosses a potential slip surface mobilizes additional shear resistance and changes the stress distribution in the soil mass, so that deformation is limited and progressive failure is delayed. Its efficiency has been shown analytically, numerically, in centrifuge tests and in the laboratory for cohesive and heterogeneous slopes under static, cyclic and drawdown conditions [2–7, 9–11]. The outcome depends on pile spacing and stiffness, on where the piles are placed and how deep they are embedded below the slip surface, on the soil properties and on the pile–soil interaction [2, 3, 6, 10, 31].

For transport infrastructure the issue is especially pressing, because embankments are loaded again and again by vehicles and trains. Cyclic loading alters the stress state of the soil, accumulates deformation and can gradually erode the margin of stability [4, 5, 13, 16, 18]. Numerical and experimental work indicates that reinforcement improves load transfer and reduces differential deformation in embankments [6, 7, 11], and geosynthetic and pile-supported systems have been studied as means of improving embankment performance under repeated and long-term loading [1, 6, 7, 11].

Field surveys show that the problem is far from academic. Along the Western Europe – Western China International Transport Corridor in the Zhambyl Region, Shalkarov [22] found widespread defects where road approaches meet bridges. He linked them mainly to poor compaction of the embankment soil, increased moisture, infiltration of flood and surface water, capillary rise, the stiffness contrast between the bridge and the approach embankment, seasonal freezing and thawing, and drainage failures. Once a step forms between the embankment and the rigid structure, passing vehicles produce impact and dynamic loads that aggravate the damage [22–24].



Fig. 1. Roadway defects at the junction of the approach embankment with the bridge (Zhambyl Region, Kazakhstan, 2018; reproduced from [22])

The usual picture is a step (bridge bump) in front of the abutment, a settled and cracked pavement, a deformed approach slab with voids beneath it and a distorted longitudinal profile (Fig. 1). These defects concern not only the structure itself; they also worsen ride quality and traffic safety [29].

Issue No. 3 · 2026
ADVANCED STUDIES
IN ARCHITECTURE AND CIVIL ENGINEERING
(ASACE)
ISSN 3134-8475 (Print)
ISSN 3134-8483 (Online)

The issue is serious enough in Kazakhstan that in 2022 recommendations R RK 218-193-2022 “Recommendations on the design of interfaces of road bridges, overpasses and artificial structures with an approach embankment” were introduced [30]. They cover construction, reconstruction and overhaul of junctions between bridges or other artificial structures and the road. Experience abroad is similar: differential settlement and deformation of transport embankments continue to limit serviceability.

In Texas, USA, surveys of bridges in Quanah, Arlington and Cleburne and of the US-67 bridge over SH-174, whose approach embankment is about 12.2 m high, named three main causes of approach settlement: voids beneath the slab, erosion and compressible fill. Settlement turns into differential settlement, then into a bump, and the bump in turn raises dynamic impact loads (Fig. 2) [24].



Fig. 2. Roadway defects at the junction of the approach embankment with the bridge (USA, Texas [24]; WSDOT photograph [Authors materials], 2000–2010)

According to a review of bridge-approach settlement studies, deformation is governed mainly by foundation conditions, backfill properties, consolidation of the embankment, the behavior of the approach slab and the bridge–embankment interface [23]. Geosynthetic reinforced soil – integrated bridge systems have been suggested as one way to ease these problems [28].

In Thailand, a bridge approach built on soft Bangkok Clay settled by about 1.35 m before it was rehabilitated, which shows how strongly consolidation and ground subsidence can drive excessive differential deformation [25].

The bridge itself rested on deep foundations, so the soft clay under the approach embankment consolidated while the bridge did not move. The approach zone was rebuilt with part of the backfill replaced by lightweight EPS geofoam, and its later behavior was examined with three-dimensional numerical modelling (Fig. 3) [25].



Fig. 3. Installation of EPS geofoam for mitigation of bridge approach settlement (Bangkok, Thailand; reproduced from [25])

Issue No. 3 · 2026
ADVANCED STUDIES
IN ARCHITECTURE AND CIVIL ENGINEERING
(ASACE)
ISSN 3134-8475 (Print)
ISSN 3134-8483 (Online)



Fig. 4. Defects on the Bhubaneswar road-over-bridge (India; reproduced from [26])

In India, a road-over-bridge near IIT Bhubaneswar with an approach embankment about 10 m high showed pronounced bumps caused by settlement of the embankment and voids beneath the approach slab. Once the void exceeded roughly 2.5 m in length, the calculated bending moment was larger than the existing slab could carry (Fig. 4) [26]. In northern New South Wales, Australia, a bridge approach on deep soft soils kept settling even after preloading, prefabricated vertical drains and later slab jacking – a reminder of how hard it is to predict long-term embankment deformation (Fig. 5) [27].

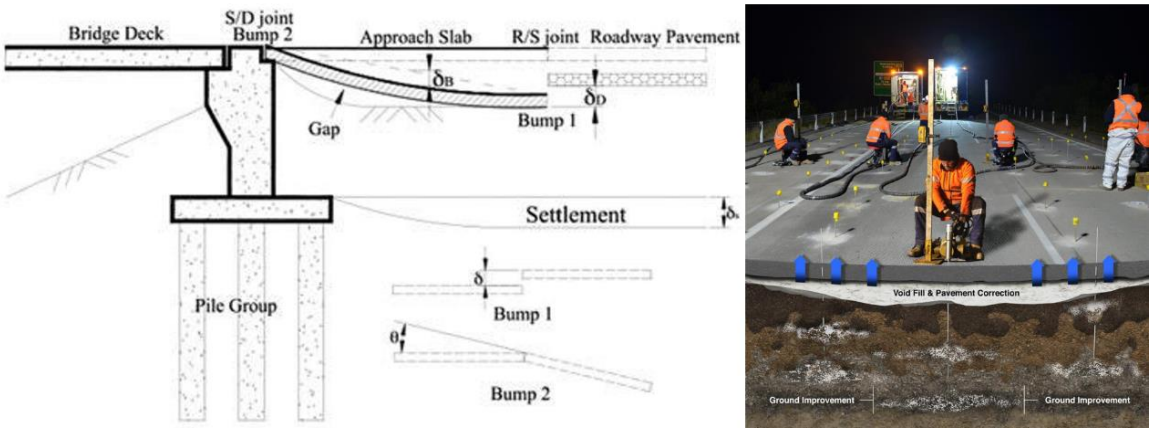


Fig. 5. Bridge approach settlement in northern New South Wales, Australia, following construction on soft ground (reproduced from [27])

Table 1. Reported defects and causes of deformation in bridge approaches and embankments

Year	Country / Site	Defect	Cause	Quantitative indicator
2018	Kazakhstan, Zhambyl Region [22]	Settlements, cracks, potholes, pavement breaks, rutting	Moisture increase, insufficient compaction	Up to 80 %
2018	Kazakhstan, Western Europe–Western China International Transport Corridor [22]	Severe defects at bridge approaches	Differential settlement	>50% of structures affected by defects
2000s–2010s	USA, Texas [24]	Bump, settlement, voids, erosion	Compressible backfill, erosion	Field case studies

ISSN 3134-8475 (Print)
ISSN 3134-8483 (Online)

2000s	USA, US-67/SH-174 [24]	Differential settlement	Clayey embankment fill	Embankment height: 12.2 m
2010	USA, Quanah/Arlington/Cleburne [24]	Bridge approach settlement	Voids, erosion, compressibility	Investigation of several bridges
2000–2015	Thailand, Bangkok [25]	Bridge approach settlement	Soft clay, consolidation	Up to 1.35 m
2024	India, Bhubaneswar [26]	Bump, voids beneath approach slab	Embankment settlement	Void >2.5 m — critical case
2025	Australia, New South Wales [27]	Approach slab settlement	Residual settlement of soft foundation soil	Exceedance of the serviceability limit

Soil properties matter just as much for reinforced slopes. Tests on cohesive and coarse-grained soils show that shear strength parameters, including their dependence on the loading path, have to be determined properly before the stability of a soil mass or structure can be judged [8, 19]. Kazakh studies have likewise pointed to the role of pile foundations and soil-strengthening technologies for structures in seismic and geologically complex conditions [20, 21]. Reinforcement, in other words, cannot be assessed apart from the actual mechanical behavior of the soil it is placed in.

Centrifuge tests, numerical and analytical models and laboratory experiments have all confirmed that piles stabilize slopes [2–7, 9–11]. Small-scale physical tests in which the dynamic response of a pile-reinforced embankment slope is measured directly under controlled vibration have received much less attention. What is missing in particular are experiments that observe the deformation of a model slope and, at the same time, record its dynamic response digitally. For transport infrastructure in seismic regions this gap matters, because the onset of instability there may depend on how soil properties, reinforcing elements and dynamic loading act together.

Digital monitoring has become a standard source of objective information on the dynamic state of structures. Modern sensors and signal processing allow vibration to be recorded and analyzed in the time and frequency domains, and vibration diagnostics have already been used to assess the response of railway and bridge structures under operational loads [12, 13, 15]. Data of this kind can also be used to calibrate and verify numerical models and to identify the dynamic parameters that control behavior.

Several questions nevertheless remain open. Much of the published work relies on centrifuge experiments or numerical modelling, so directly measured dynamic-response data from controlled laboratory tests are scarce [2–7]. The joint effect of dynamic excitation and reinforcement layout on the observed onset of slope instability has rarely been examined. And digital vibration monitoring is still seldom built into experimental assessments of pile-reinforced slopes. Taken together, these points call for an approach that links physical modelling, controlled excitation and digital monitoring.

The gap addressed here is therefore the shortage of experimental data on pile–soil interaction in an embankment slope under controlled dynamic loading with simultaneous digital recording of the vibration response. What is new in this study is a direct comparison of an unreinforced and a pile-reinforced small-scale embankment slope tested under the same controlled vibration and monitored by accelerometers. We pay particular attention to how instability develops as the frequency increases and to the response recorded by the sensors.

The tests use a physical model of an embankment slope and a laboratory vibration

Issue No. 3 · 2026
ADVANCED STUDIES
IN ARCHITECTURE AND CIVIL ENGINEERING
(ASACE)
ISSN 3134-8475 (Print)
ISSN 3134-8483 (Online)

platform that reproduces controlled dynamic loading. Digital accelerometers record the response, and ZETLAB is used to acquire and process the signals. From the results we identify the excitation at which instability begins and evaluate how effective the pile-and-beam reinforcement is. The same test and monitoring scheme may be useful for assessing slope stability and designing monitoring of transport embankments and other geotechnical structures exposed to dynamic, including seismic, loading.

2 METHODS AND MATERIALS

The field cases above show that differential settlement and dynamic deformation at bridge approaches are tied to the condition and stability of the approach embankment and its slopes. For this reason the experiments deal with a simplified physical model of an embankment slope under controlled dynamic excitation; the abutment and the approach slab are not reproduced. In practice, embankment slopes are stabilized with vegetation [14], by compacting the soil or by building retaining structures in the zone of possible sliding. Retaining walls and rows of piles resist the sliding mass mechanically (Fig. 6). Piles are chosen where a retaining wall is impractical, and they may be timber, concrete, reinforced concrete or steel. They carry the lateral pressure of the sliding soil down to stable ground below the slip surface; how many piles are needed and how far apart they stand follow from the lateral force on each pile, which in turn depends on soil strength, pile diameter and spacing [2, 3, 31].

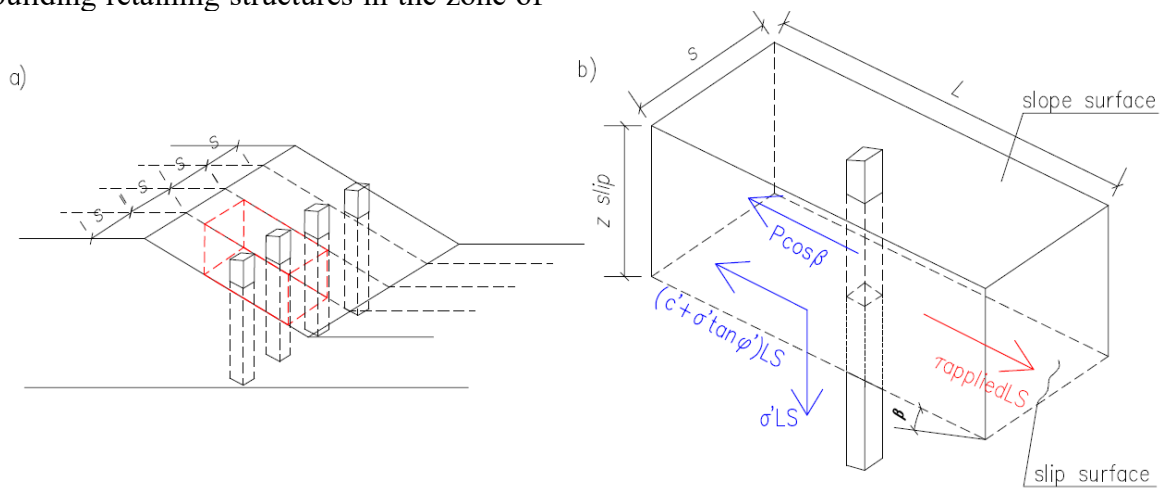


Fig. 6. Sliding mechanism of a slope reinforced with piles: a – general view; b – forces acting on the soil stabilized by piles

The experiment had two aims: to find out how effective piles tied by beams are in strengthening a soil slope under vibration that simulates seismic excitation, and to collect response data for the unreinforced and reinforced slopes that can support further development of the method for existing and new embankments in seismic areas.

The model represented an embankment slope with a surcharge on the crest standing in for a structure. It was tested twice, without and with pile reinforcement, on the seismic platform of the Geotechnics Laboratory at the Kazakh Leading Academy of Architecture and Civil Engineering. The platform is a welded steel frame, 0.9 × 1.0 m in plan, resting on springs. A rotating eccentric (unbalanced-mass) exciter, driven through a vector frequency converter, sets it into harmonic oscillation at a chosen frequency.

The exciting force of such an exciter is $F = m_e \cdot e \cdot \omega^2$, where m_e is the unbalanced mass, e its eccentricity and $\omega = 2\pi f$. The force amplitude thus rises with the square of the

Issue No. 3 · 2026
ADVANCED STUDIES
IN ARCHITECTURE AND CIVIL ENGINEERING
(ASACE)
ISSN 3134-8475 (Print)
ISSN 3134-8483 (Online)

frequency f, and between 8 and 10 Hz it grows by a factor of $(10/8)^2 \approx 1.56$. The spring-mounted platform also has a natural frequency of its own, so frequency and intensity of excitation cannot be varied independently in this set-up. For this reason the results are discussed in terms of both the frequency and the measured accelerations (Section 3).

2.1 Description of the test bench

The prototype we have in mind is a structure standing at the crest of an embankment slope. A strong earthquake may cause the slope to lose stability and slide, putting the structure at risk. In the reinforced case, piles tied at their heads by beams form a spatial lattice; it raises the shear resistance of the soil and with it the stability of both the slope and the structure.

The soil was placed in a box of 9 mm plexiglass with internal dimensions. Aluminium angles and mounting adhesive stiffened the corners. Because the walls are transparent, the deformation of the slope could be watched during the tests (Fig. 7) .



Fig. 7. Model of the soil embankment slope installed on the seismic platform

Connecting bolts fixed the box rigidly to the platform. We used loam as the model soil: it is a common embankment fill, and its weak cohesion lets slope deformation develop at the excitation levels the platform can deliver. The soil was placed in layers, each layer being compacted. The bulk density, water content, dry density, grain-size composition, plasticity index, cohesion and angle of internal friction of the placed soil were determined in the laboratory, the shear parameters by direct shear (cf. [8]). Values for loams from SP RK 5.01-102-2013 “Soil bases of buildings and structures” [32] served only as a reference for comparison.

The slope was formed at roughly 45°. That is steeper than the slopes of ordinary road embankments; we chose it on purpose so that the model stood close to its limit static state and could be brought to failure within the platform’s range. A rigid model foundation of 20 kg was set on the crest to represent a structure on the embankment. The surcharge adds to the driving forces in the slope and lets us see how the system reacts to vertical and inertial loads.

With the soil and surcharge in place, two three-component digital accelerometers ZET 7152-N (Fig. 8), designed for vibration monitoring of structures and soil foundations, were installed in the model (Figs. 9 and 10). Sensor 1 recorded channels 20, 21 and 22 (X, Y and Z), and sensor 2 channels 25, 26 and 27. The Z axis is vertical; X and Y are horizontal. Signals were sampled at 50 Hz (time step 0.02 s), which is adequate for excitation up to 10 Hz

Issue No. 3 · 2026
ADVANCED STUDIES
IN ARCHITECTURE AND CIVIL ENGINEERING
(ASACE)
ISSN 3134-8475 (Print)
ISSN 3134-8483 (Online)



Fig. 8. ZET 7152-N digital accelerometer

2.2 Description of the experiment. The first stage of testing

The unreinforced slope was tested first and served as the reference case (Fig. 9). The test took about 90 s.

The frequency converter raised the excitation frequency gradually from 1 to 8 Hz, on average by about 0.1 Hz/s. At roughly 70 s, when 8 Hz was reached, the slope started to slide and carried the surcharge model with it.

The frequency was then brought back to zero and the platform left to oscillate freely until it stopped. We judged the onset of instability visually, through the transparent wall and from photographs, as the moment the soil began to move visibly down the slope; displacements were not measured with instruments.



Fig. 9. Test model with sensors installed in the soil embankment without slope reinforcement: on the left – before the first test; on the right – after the first test (at 70 s)

Before the second stage, the soil was removed and re-placed using the same procedure as in the first test. The slope was then reinforced with timber piles joined at their heads by timber beams (Fig. 10). At this scale the piles could simply be pushed into the soil instead of being driven. They were 10 cm long and spaced 6 cm apart. The piles extended below the potential slip surface, which we estimated from the failure surface seen in the first test.

The lattice of beams had 12 spans along the slope and 3 spans down the slope, laid parallel to its face.

Issue No. 3 · 2026
ADVANCED STUDIES
IN ARCHITECTURE AND CIVIL ENGINEERING
(ASACE)
ISSN 3134-8475 (Print)
ISSN 3134-8483 (Online)



Fig. 10. Test model with sensors installed in the soil embankment with the reinforced slope: on the left – before the second test; on the right – after the second test

The second stage of testing

The reinforced model was tested the same way, except that the frequency was raised from 1 to 10 Hz. It reached 8 Hz at about 50 s (≈ 0.14 Hz/s on average) and 10 Hz at about 70 s (≈ 0.1 Hz/s between 8 and 10 Hz). The ramp rates of the two tests therefore differed, and the reinforced slope experienced 8 Hz and more for about 20 s before it failed.

At about 70 s and close to 10 Hz the oscillations became strong; the slope began to collapse and the piles were exposed (Fig. 11). We then switched off the exciter and let the platform come to rest.

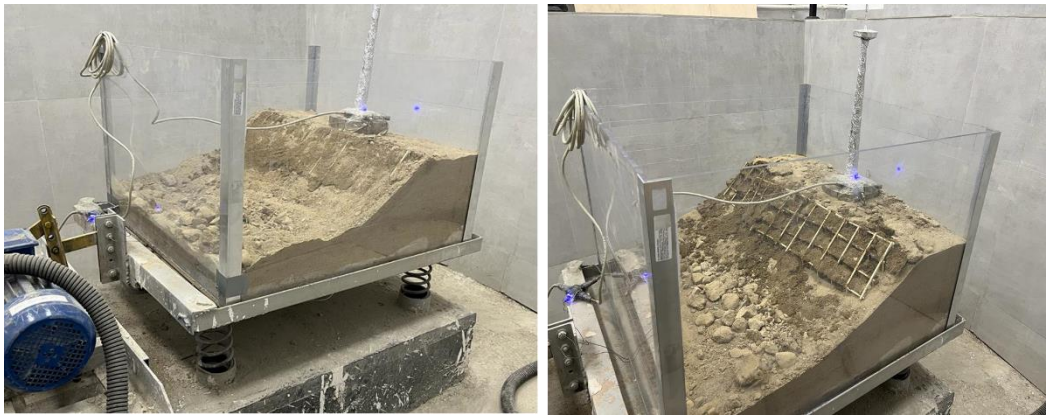


Fig. 11. Result of the second stage of testing of the soil embankment slope reinforced with piles: on the left – at 50 s (≈ 8 Hz); on the right – at 70 s (≈ 10 Hz)

3 RESULTS AND DISCUSSION

Accelerations (Figs. 12 and 13) were recorded with ZETLAB, which displays, stores and processes the signals in real time, so the data could be checked while each test was running.

Issue No. 3 · 2026
ADVANCED STUDIES
IN ARCHITECTURE AND CIVIL ENGINEERING
(ASACE)
ISSN 3134-8475 (Print)
ISSN 3134-8483 (Online)

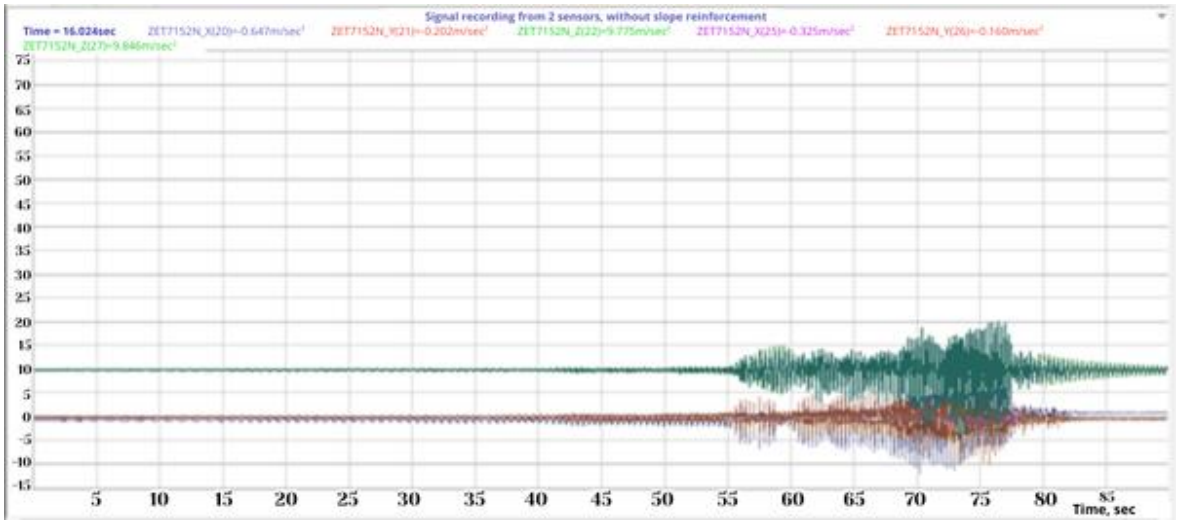


Fig. 12. Acceleration records of the first test (unreinforced slope)

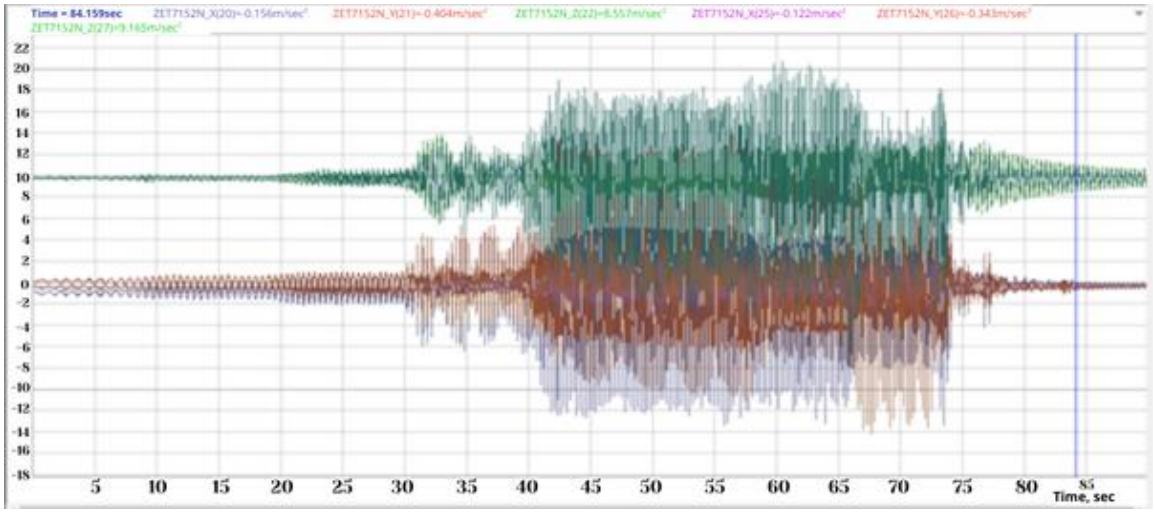


Fig. 13. Acceleration records of the second test (pile-reinforced slope)

Tables 2 and 3 summarize the records of the first (unreinforced) and second (reinforced) tests, for the whole record and for the part shown in Figs. 12 and 13. The vertical channels (22 and 27) have mean values of about 9.7 m/s²: the sensors include gravity in their output, so the vertical dynamic response is better described by the standard deviation than by the mean or RMS. Statistics of the time column say nothing beyond the record length and are left out. The software also exported "fundamental frequency" values of 0.04–0.12; these have nothing to do with the 1–10 Hz excitation and are not the natural frequency of the system, so we removed them.

Table 2. Statistics of the acceleration records of the first test (unreinforced slope)

Data	X	Y1	Y2	Y3	Y4	Y5	Y6
	Time	ZET7152N _X(20)	ZET7152N _Y(21)	ZET7152N _Z(22)	ZET7152N _X(25)	ZET7152N _Y(26)	ZET7152N _Z(27)
	Seconds	m/s^2	m/s^2	m/s^2	m/s^2	m/s^2	m/s^2
For all data							
Minimum value	0.000000	-12.094400	-5.359920	4.476220	-4.205680	-10.416000	-5.251400

ISSN 3134-8475 (Print)
ISSN 3134-8483 (Online)

Maximum value	89.980003	6.081340	9.084870	15.078900	3.016700	7.274630	10.125799
Arithmetic mean	–	-0.547543	-0.215375	9.753019	-0.399471	-0.422499	9.763654
Root mean square (RMS) value	–	1.891900	1.272531	9.808423	0.666861	1.255939	9.976084
Standard deviation (SD)	–	1.811135	1.254312	1.041159	0.534032	1.182873	2.047982
For the visible part							
Minimum value	0.000000	-12.094400	-5.359920	4.476220	-4.205680	-10.416000	-5.251400
Maximum value	87.800003	6.081340	9.084870	15.078900	3.016700	7.274630	10.125799
Arithmetic mean	–	-0.579722	-0.203097	9.753175	-0.399453	-0.423018	9.762977
Root mean square (RMS) value	–	1.911541	1.283307	9.809175	0.671952	1.269789	9.980485
Standard deviation (SD)	–	1.821720	1.267279	1.046778	0.540392	1.197391	2.072522

Table 3. Statistics of the acceleration records of the second test (pile-reinforced slope)

Data	X	Y1	Y2	Y3	Y4	Y5	Y6
	Time	ZET7152N_X(20)	ZET7152N_Y(21)	ZET7152N_Z(22)	ZET7152N_X(25)	ZET7152N_Y(26)	ZET7152N_Z(27)
	Seconds	m/s^2	m/s^2	m/s^2	m/s^2	m/s^2	m/s^2
For all data							
Minimum value	0.000000	-13.403700	-6.791880	4.132020	-5.158600	-14.187100	-7.390720
Maximum value	89.980003	5.639180	14.011400	13.961200	3.339150	9.604730	10.757000
Arithmetic mean	–	-0.603727	0.011970	9.741151	-0.404566	-0.415231	9.623785
Root mean square (RMS) value	–	3.059556	2.969586	9.811969	1.032892	2.396810	10.269970
Standard deviation (SD)	–	2.999733	2.969892	1.176870	0.950470	2.360830	3.585793
For the visible part							
Minimum value	0.000000	-13.403700	-6.791880	4.132020	-5.158600	-14.187100	-7.390720
Maximum	89.940002	5.639100	14.011400	13.961200	3.339150	9.604730	10.757000

ISSN 3134-8475 (Print)
ISSN 3134-8483 (Online)

value							
Arithmetic mean	–	-0.603808	0.012039	9.740785	-0.404504	-0.415158	9.623569
Root mean square (RMS) value	–	3.060224	2.970244	9.811622	1.033058	2.397311	10.270041
Standard deviation (SD)	–	3.000398	2.970550	1.177003	0.950677	2.361352	3.586576

The main observations from the tests are as follows:

1. First test, unreinforced slope. Sliding and displacement began when the frequency reached 8 Hz. With the surcharge on its crest, the unreinforced slope was not stable enough for the applied dynamic loading.

2. Second test, pile-reinforced slope. The slope and the piles started to fail only under strong oscillations at the highest frequency, about 10 Hz. The reinforcement thus moved the onset of instability to a higher level of excitation. Table 4 compares both tests at their maximum frequencies.

Table 4. Comparison of the test results at the maximum excitation frequencies

Experimental results	Test 1, unreinforced slope	Test 2, pile-reinforced slope
Maximum excitation frequency	8 Hz	≈ 10 Hz
Surcharge mass	20 kg	20 kg
Time of onset of instability	≈ 70 s	≈ 70 s
Soil	Loam	Loam
Peak absolute acceleration, sensor 2, X (channel 25)	4.21 m/s²	5.16 m/s²
Peak absolute acceleration, sensor 2, Y (channel 26)	10.42 m/s²	14.19 m/s²
Peak absolute acceleration, sensor 1, X (channel 20)	12.09 m/s²	13.40 m/s²
Peak absolute acceleration, sensor 1, Y (channel 21)	9.08 m/s²	14.01 m/s²

At about 10 Hz the reinforced model gave higher peak accelerations than the unreinforced one at 8 Hz: about 1.23 times higher in channel 25 and 1.36 times in channel 26 (sensor 2), and 1.11 and 1.54 times in channels 20 and 21 (sensor 1) (Table 4). Channels 25 and 26 of sensor 2 are taken as the main indicators. These values are response accelerations of the model, not of the input motion. Between 8 and 10 Hz the exciting force grows by about 1.56 times, so the higher peaks in the second test are mainly due to the stronger excitation, possibly together with the greater stiffness of the reinforced soil, and cannot by themselves be taken as a measure of load-bearing capacity. A more rigorous interpretation would require the amplification factor of the model with respect to the platform.

The two tests are now compared at the same excitation frequency of 8 Hz (Table 5).

Issue No. 3 · 2026
ADVANCED STUDIES
IN ARCHITECTURE AND CIVIL ENGINEERING
(ASACE)
ISSN 3134-8475 (Print)
ISSN 3134-8483 (Online)

Table 5. Comparison of the test results at an excitation frequency of 8 Hz

Experimental results	Test 1, unreinforced slope	Test 2, pile-reinforced slope
Excitation frequency	8 Hz	8 Hz
Surcharge mass	20 kg	20 kg
Time at which 8 Hz was reached	≈ 70 s	≈ 50 s
Onset of significant deformation	≈ 70 s (at 8 Hz)	not observed at 8 Hz (≈ 70 s, ≈ 10 Hz)
Soil	Loam	Loam
Peak absolute acceleration, X (channel 25)	4.21 m/s²[a]	3.99 m/s²[b]
Peak absolute acceleration, Y (channel 26)	10.42 m/s²[a]	10.11 m/s²[b]

Note: [a] extreme value over the whole record up to failure; [b] extreme value within the record fragment 49.88–50.14 s (Table 6).

In the second test 8 Hz was reached at about 50 s; Table 6 lists the corresponding part of the record. In this window the peak absolute accelerations were 3.99 and 10.11 m/s² in channels 25 and 26 (sample 2502, t = 50.02 s), and 11.53 and 12.34 m/s² in channels 20 and 21 of sensor 1. They are close to the values at which the unreinforced model failed (Table 5), yet the reinforced slope stayed stable (Fig. 11, left). The comparison is only indicative, though: for the unreinforced model we used extremes over the whole record, for the reinforced one extremes over a 0.26 s window. Peak and RMS values over windows of equal length at 8 Hz in both records would make the comparison strict.

Table 6. Fragment of the acceleration record of the second test (pile-reinforced slope) at about 50 s (excitation frequency ≈ 8 Hz)

Sample no.	X	Y1	Y2	Y3	Y4	Y5	Y6
	Time	ZET7152N_X(20)	ZET7152N_Y(21)	ZET7152N_Z(22)	ZET7152N_X(25)	ZET7152N_Y(26)	ZET7152N_Z(27)
	Seconds	m/s²	m/s²	m/s²	m/s²	m/s²	m/s²
2495	49.88	3.28399	-5.76641	8.76657	-1.03576	2.06854	15.4055
2496	49.9	4.75175	-5.14832	10.0472	2.13512	4.77107	14.6901
2497	49.92	5.08808	-3.11882	9.42418	1.97102	1.56754	13.6275
2498	49.94	4.69885	-4.00247	9.74257	0.62652	1.33541	17.4832
2499	49.96	2.98306	-2.73298	8.52629	0.362012	-0.033412	16.278
2500	49.98	0.739894	-0.184161	9.1103	-0.922529	-0.82018	16.7338
2501	50	0.261613	0.303031	8.85403	0.574464	-2.06746	4.33787
2502	50.02	-1.42146	0.632408	10.0707	-3.99327	-10.11	4.08228
2503	50.04	-3.84443	1.54246	11.6982	-2.48282	-0.667633	6.47974
2504	50.06	-9.0694	7.47658	9.17067	0.819962	-0.255839	-1.37323
2505	50.08	-11.5291	12.3412	7.90145	-2.02852	-1.52797	4.96547
2506	50.1	-2.57393	2.65535	11.8269	0.206027	2.77686	2.96823
2507	50.12	2.54246	-4.45289	10.9682	-1.87548	-1.83047	8.64681
2508	50.14	3.27487	-5.66618	8.77468	-0.925391	2.30328	16.4901

Note: sampling frequency 50 Hz (time step 0.02 s). Largest absolute values in the fragment, at sample 2502 (t = 50.02 s): 3.99 m/s² in channel 25 (X) and 10.11 m/s² in channel 26 (Y).

The two tests gave markedly different results, although the type of dynamic loading was the same. Without reinforcement, the slope began to move at 8 Hz. Being steep and loaded at the crest, it had little reserve against

ISSN 3134-8475 (Print)
ISSN 3134-8483 (Online)

the applied vibration, and the shear resistance of the soil alone could not keep it stable.

With rows of piles tied by beams, the slope sustained 8 Hz at response accelerations close to those that had caused failure of the unreinforced slope (Table 5). This agrees with the mechanism in Fig. 6: the piles cross the potential slip surface and transfer part of the driving force of the sliding mass to stable soil below, while the head beams distribute the load so that the pile lattice acts as a single unit. Centrifuge tests of pile-reinforced slopes indicate the same mechanism [2, 3, 9].

The reinforced model failed at about 10 Hz, where the exciting force is roughly 1.56 times greater than at 8 Hz, i.e. the reinforced slope withstood a considerably stronger excitation. The higher response accelerations at failure (Table 4) should be interpreted with caution: they may result from the stronger excitation, from a change in stiffness of the reinforced system, or from both, and do not by themselves quantify bearing capacity.

The observations can be placed in an engineering context using the pseudo-static approach, where the seismic action is represented by a horizontal inertial force $k_h \cdot W$ with $k_h = a/g$ [33, 34]. At the onset of instability of the unreinforced slope, the peak response accelerations of 4.2 m/s² (X) and 10.4 m/s² (Y) in channels 25 and 26 give $k_h \approx 0.43$ and 1.06. By comparison, the MSK-64 scale adopted for seismic zoning in Kazakhstan [35] assigns peak ground accelerations of 2–4 m/s² to intensity 9 and 4–8 m/s² to intensity 10. These values cannot be applied to real embankments directly, since they are response accelerations of a 1g model, not input motions, and the stress level in the model is much lower than in a prototype.

The comparison is qualitative and subject to several limitations. (i) Only one test was run per configuration, so the scatter due to soil placement is unknown, and the difference of about 2 Hz between the thresholds needs confirmation by repeated tests. (ii) At 1g, stresses in the model are orders of magnitude lower than in a prototype and soil strength does not scale like geometry [36, 37]; applying the results to full-scale embankments requires further work. (iii) Failure was determined visually, without displacement measurements. (iv) The rigid box walls may reflect waves and add friction, both of which affect the response. (v) Frequency and intensity of excitation were not controlled separately.

Within these limits, the pile-and-beam reinforcement made the model slope more stable under vibration simulating seismic excitation and pushed the onset of instability to a higher excitation level.

4 CONCLUSIONS

1. We examined experimentally how well rows of piles connected by beams reinforce a road embankment slope under vibration that simulates seismic excitation.

2. On the seismic platform the unreinforced slope began to slide at 8 Hz, while the reinforced slope held at 8 Hz with response accelerations of the same order and lost stability only near 10 Hz. Because the force of the unbalanced-mass exciter grows with the square of frequency, failure of the reinforced slope required an excitation about 1.56 times more intense, which points to a positive effect of the pile-and-beam reinforcement.

3. Recording the response synchronously with three-component digital accelerometers and processing it in ZETLAB allowed us to link the visually observed onset of instability to measured accelerations. The higher peaks at failure of the reinforced model (up to 5.2 and 14.2 m/s², compared with 4.2 and 10.4 m/s²) reflect mainly the stronger excitation and should not be taken as a direct measure of bearing capacity.

4. The findings are qualitative and comparative: each configuration was tested once at 1g and failure was judged visually.

ISSN 3134-8475 (Print)
ISSN 3134-8483 (Online)

They do not transfer directly to full-scale embankments, but they give a starting point for further experiments and for calibrating numerical models of transport embankments in seismic regions.

5. The work adds experimental evidence, obtained with digital vibration monitoring, on how pile reinforcement affects the seismic stability of soil slopes, and in this way supports the development of methods for seismic strengthening of earth structures.

6. Next steps include repeated tests with controlled density and moisture of the soil, measurement of platform (input) acceleration and of displacements, spectral analysis of the records, different pile spacing, length and embedment, other soils, attention to scaling laws, and comparison with pseudo-static and numerical analyses.

REFERENCES

REFERENCES

1. Luo, F., Huang, R., Zhang, G. Centrifuge modeling of the geogrid-reinforced slope subjected to differential settlement. *Acta Geotechnica.* 2020; 15(10): 3027–3040. https://doi.org/10.1007/s11440-020-01010-x

2. Ma, L., Yang, K., Yuan, W., Li, L., Wei, Y., Ma, C., et al. Centrifuge modeling of the pile foundation reinforcement on slopes subjected to uneven settlement. Bulletin of Engineering *Geology and the Environment.* 2020; 79(5): 2647–2658. https://doi.org/10.1007/s10064-020-01723-z

3. Liu, X., Luo, G., Zhang, L. Pile reinforcement behavior and mechanism in a soil slope under drawdown conditions. *Bulletin of Engineering Geology and the Environment.* 2021; 80: 4097–4109. https://doi.org/10.1007/s10064-021-02191-9

4. Rehman, A.U., Zhang, L. Cyclic behavior of gravel–steel interface under varying rotational shear paths. *Canadian Geotechnical Journal*. 2021; 58(3): 305–316. https://doi.org/10.1139/cgj-2019-0472

5. Chen, T., Luo, F., Zhang, G., Yang, Y. Study on deformation and failure of slopes under coupled application of water level change and vertical load. *Bulletin of Engineering Geology and the Environment.* 2021; 80(1): 353–364. https://doi.org/10.1007/s10064-020-01958-w

6. Phutthananon, C., Jongpradist, P., Dias, D., Jamsawang, P. Numerical study of the deformation performance and failure mechanisms of TDM pile-supported embankments. *Transportation Geotechnics*. 2021; 30: 100623. https://doi.org/10.1016/j.trgeo.2021.100623

7. Pham, T.A., Tran, Q.A., Villard, P., Dias, D. Geosynthetic-reinforced pile-supported embankments-3D discrete numerical analyses of the interaction and mobilization mechanisms. *Engineering Structures*. 2021; 242: 112337. https://doi.org/10.1016/j.engstruct.2021.112337

8. Bondar, I.S. Shift tests of cohesive soils under the various loading trajectories [Sdvigoviye ispitaniya syaznyh gruntov pri razlichnyh traektoriyah nagrujeniya]. *Magazine of Civil Engineering*. 2012; 7(33): 50–57. file:///D:/ЗАГРУЗКИ/Shift_tests_of_cohesive_soils_under_the_various_lo.pdf (In Russ.)

9. Liu, S., Zhang, G., Luo, F. Centrifuge modeling of new pile reinforcement on slopes subjected to drawdown. *Bulletin of Engineering Geology and the Environment*. 2022; 81(10): 396. https://doi.org/10.1007/s10064-022-02893-8

10. Cheng, Y.M., et al. Stability of expansive soil slopes reinforced with anchor cables based on rotational-translational mechanisms. *Computers and Geotechnics*. 2022; 146: 104747. https://doi.org/10.1016/j.compgeo.2022.104747

11. Ikbarieh, A., Izadifar, M.A., Abu-Farsakh, M.Y., Voyiadjis, G.Z. A parametric study of

ISSN 3134-8475 (Print)
ISSN 3134-8483 (Online)

embankment supported by geosynthetic reinforced load transfer platform and timber piles tip on sand. *Transportation Geotechnics*. 2023; 38: 100901. https://doi.org/10.1016/j.trgeo.2022.100901

12. Bondar, I.S., Aldekeyeva, D.T., Ospanova, Z.K. Stress-strain states of reinforced concrete spans of a railroad overpass using a spatial finite element model. *Vibroengineering Procedia*. 2024; 54: 320–326. https://doi.org/10.21595/vp.2024.24086

13. Bondar, I.S., Karibaeva, G.B., Kurbenova, A.K. Vibration diagnostics of transportation structures on railroads. *Vibroengineering Procedia.* 2024; 54: 109–115. https://doi.org/10.21595/vp.2024.24093

14. Yazdani, F., AliPanahi, P., Sadeghi, H. A comparative study of environmental and economic assessment of vegetation-based slope stabilization with conventional methods. *Journal of Environmental Management.* 2024; 359: 121002. https://doi.org/10.1016/j.jenvman.2024.121002

15. Bondar, I.S., Jexenbaev, E.K., Uteshbaeva, A.A., Uskembaeva, B.O., Abiev, B.A. Experimental studies of dynamic properties of soils of railroad embankments. *Vibroengineering Procedia*. 2025; 58: 24–30. https://doi.org/10.21595/vp.2025.24943

16. Luo, F., Zhang, G. New method for full-process deformation of slopes subject to drying-wetting cycles. *Bulletin of Engineering Geology and the Environment.* 2025; 84(5): 239. https://doi.org/10.1007/s10064-025-04261-8

17. Liu, S., Luo, F., Zhang, G. New simplified stability analysis method of structuralized cemented slopes. *Acta Geotechnica*. 2025; 20(1): 23–36. https://doi.org/10.1007/s11440-024-02495-6

18. Ospanova, Z.K., Aldekeyeva, D.T., Bondar, I.S., Belov, A.G., Baratova, T.S., Al-Dulaimi, S.D.S. Dynamic analysis of the stress-strain state of a beam superstructure of a railway bridge under moving train loads. *Vibroengineering Procedia*. 2026; 64: 1–5. https://doi.org/10.21595/vp.2026.26503

19. Khomyakov, V.A., Sagybekova, A.O. Strength problems of coarse-grained soils based on results of shear tests. *Vestnik KazGASA*. 2007: 127–131. (In Russ.)

20. Khomyakov, V.A., Samat, A.S. Seismic protection of buildings using pile foundations. *Vestnik KazGASA*. 2019; (1): 175. (In Russ.)

21. Dzhumadilova, S.Zh., Khomyakov, V.A., Kuanyshbai, M.A. Technology for strengthening soil materials using two-component polyurethane material GEOPUR. *QazBSQA Bulletin. Architecture*. 2024; 1(91): 65–75. https://doi.org/10.51488/1680-080X/2024.1-05 (In Russ.)

22. Shalkarov, A.A. Defects in the interface of the carriageway with the bridge and the causes of their formation. *Industrial Transport of Kazakhstan*. 2018; 4(61): 27–31. (In Russ.)

23. Prakash, B., Tiwari, A.K., Dash, S.R. Bridge approach settlement and its mitigation schemes: a review. *Transportation Research Record*. 2024; 2678(8): 660–689. https://doi.org/10.1177/03611981231220630

24. Puppala, A.J., Archeewa, E., Saride, S., Nazarian, S., Hoyos, L. Recommendations for design, construction, and maintenance of bridge approach slabs. Report No. FHWA/TX-11/0-6022-2. Arlington (TX): *University of Texas at Arlington*; 2012.

25. Malai, A., Youwai, S., Watcharasawe, K., Jongpradist, P. Bridge approach settlement mitigation using expanded polystyrene foam as light backfill: case study and 3D simulation. *Transportation Geotechnics*. 2022; 35: 100794. https://doi.org/10.1016/j.trgeo.2022.100794

26. Prakash, B., Tiwari, A.K., Dash, S.R., Patra, S. Structural evaluation and performance-based optimization of approach slab design for mitigating bridge approach settlement through an Indian case study. *Structures*. 2024; 60: 105864. https://doi.org/10.1016/j.istruc.2024.105864

27. Huang, S., Huang, J., Jones, M., Kamruzzaman, A.H.M., et al. Reassessment of post-construction residual settlement of a bridge approach embankment using Bayesian back analysis. *Transportation Geotechnics*. 2025; 55: 101686. https://doi.org/10.1016/j.trgeo.2025.101686

ISSN 3134-8475 (Print)
ISSN 3134-8483 (Online)

28. Abdullah, N.H.H., Ng, K.S., Jais, I.B.M., Idrus, J. Use of geosynthetic reinforced soil-integrated bridge system to alleviate settlement problems at bridge approach: a review. *Physics and Chemistry of the Earth, Parts A/B/C*. 2023; 129: 103304. https://doi.org/10.1016/j.pce.2022.103304

29. Anisimov, A.V., Rubezhansky, A.V. Determination of the evenness and safety of passage on bridge structures [Ocenka rovnosti I bezopasnosti proezda po mostovym soorujeniyam]. *News of the Kazan State University of Architecture and Engineering*. 2025; 3(73): 311–320. https://doi.org/10.48612/NewsKSUAE/73.26 (In Russ.)

30. R RK 218-193-2022. Recommendations on the design of interfaces of road bridges, overpasses and artificial structures with an approach embankment. *Astana: Committee for Roads of the Ministry of Industry and Infrastructural Development of the Republic of Kazakhstan*; 2022. (In Russ.)

31. Ito, T., Matsui, T. Methods to estimate lateral force acting on stabilizing piles. *Soils and Foundations*. 1975; 15(4): 43–59. https://doi.org/10.3208/sandf1972.15.4_43

32. SP RK 5.01-102-2013. Soil bases of buildings and structures. *Astana: Committee for Construction and Housing and Communal Services of the Republic of Kazakhstan*; 2013. (In Russ.)

33. Newmark, N.M. Effects of earthquakes on dams and embankments. *Géotechnique*. 1965; 15(2): 139–160. https://doi.org/10.1680/geot.1965.15.2.139

34. Kramer, S.L. Geotechnical earthquake engineering. *Upper Saddle River (NJ): Prentice Hall*; 1996.

35. SP RK 2.03-30-2017 (as amended). Construction in seismic zones. *Nur-Sultan: Committee for Construction and Housing and Communal Services of the Ministry of Industry and Infrastructural Development of the Republic of Kazakhstan*; 2019. (In Russ.)

36. Iai, S. Similitude for shaking table tests on soil-structure-fluid model in 1g gravitational field. *Soils and Foundations.* 1989; 29(1): 105–118. https://doi.org/10.3208/sandf1972.29.105

37. Muir Wood, D. Geotechnical modelling. *London: Spon Press*; 2004.

ISSN 3134-8475 (Print)
ISSN 3134-8483 (Online)

FUNDING

This research received no external funding.

CONFLICT OF INTEREST

The authors declare no conflict of interest.

ARTIFICIAL INTELLIGENCE STATEMENT

The authors used [tool name, version] only to edit the language and check the grammar of the manuscript. All output was checked and corrected by the authors, who bear full responsibility for the scientific content of the article, including the analyses, interpretations and conclusions.

INFORMATION ABOUT THE AUTHORS

A.A. Adiyeva – Doctoral student of the department of transport construction and urban studies, Kazakh Automobile and Road Institute named after L. B. Goncharov (KazARI), Almaty, Kazakhstan, adieva61@gmail.com, https://orcid.org/0000-0002-8513-8767
T.S. Baratova – Master's in Technical Sciences, Senior lecturer at the department of transport construction and urban studies, Kazakh automobile and road institute named after L. B. Goncharov (KazARI), Almaty, Kazakhstan, baratovatatyana1@mail.ru, https://orcid.org/0009-0000-8813-6743
I.S. Bondar – Candidate of Technical Sciences, Doctor of Philosophy, specialty «Transport Construction», Associate Professor, specialty «Civil Engineering», Professor of the Department of Transport Construction and Urban Studies, Kazakh Automobile and Road Institute named after L. B. Goncharov (KazARI), Almaty, Kazakhstan, ivan_sergeevich_08@mail.ru, https://orcid.org/0000-0001-7376-5643
A.V. Anisimov – Candidate of Technical Sciences, Associate Professor, Department of Bridges, Tunnels and Building Structures, Moscow Automobile and Road Construction State Technical University (MADI), Moscow, Russia, anisimov-ok@yandex.ru, https://orcid.org/0009-0004-7692-8574

AUTHORS CONTRIBUTION

A.A. Adiyeva – provided the project documentation; organized internships and practical training in construction; collected and analyzed project-related information.
T.S. Baratova – developed the architectural and structural solutions; prepared the computational model; analyzed seismic-resistant design solutions; processed the research results; prepared and wrote the manuscript.
I.S. Bondar – supervised the research; developed the research methodology; carried out scientific editing of the manuscript; analyzed and interpreted the results; performed the final review of the article.
A.V. Anisimov – provided scientific and methodological support; assisted in analyzing and interpreting the results; reviewed and edited the manuscript; took part in the final revision of the article.

The article was submitted 05 July 2026; approved after reviewing 25 July 2026; accepted for publication 15 August 2026.